Journal of Quantitative Spectroscopy & Radiative Transfer 131 (2013) 82–87

Contents lists available at ScienceDirect

Journal of Quantitative Spectroscopy & Radiative Transfer

journal homepage: www.elsevier.com/locate/jqsrt

Symmetry relations for the Mueller scattering matrix integrated over the azimuthal angle

Maxim A. Yurkin [a,b,*]

[a] Institute of Chemical Kinetics and Combustion SB RAS, Institutskaya Str. 3, 630090 Novosibirsk, Russia
[b] Novosibirsk State University, Pirogova Str. 2, 630090 Novosibirsk, Russia

ARTICLE INFO

Article history:
Received 2 November 2012
Received in revised form
21 November 2012
Accepted 22 November 2012
Available online 2 December 2012

Keywords:
Light scattering simulation
Symmetry
Mueller matrix
Azimuthal Fourier components

ABSTRACT

Explicit symmetry relations for azimuthal Fourier components of the Mueller scattering matrix were derived as implications of particular scatterer symmetries. Several types of the latter were considered, including plane symmetries and second- and fourth-order rotational symmetries around the z-axis. Depending on the particular symmetry the integrals of the Mueller matrix over the azimuthal angle either vanish or equal the ones computed over the reduced angular range. Derived relations provide an independent test for any computer code that computes these integrals, which was illustrated by the discrete-dipole-approximation simulations for a number of test particles. Moreover, these relations can be used to reduce the time for computing these integrals for a symmetric particle by several times, which is relevant for several specific applications.

1. Introduction

Symmetries are fundamental to the light-scattering theory. They allow one to solve the light-scattering problem for a wide variety of particle shapes: from the most symmetric shape, a sphere [1], to more complex shapes with finite-order symmetries [2,3]. Another kind of symmetry is that of the computed results, in particular, of the Mueller matrix elements [4]. Such symmetries have smaller direct utility, since the scattering problem has to be solved beforehand. However, they are more general, applying in some form to almost all kinds of scatterers, and constitute an independent test for both simulation results, e.g. [5–7], and experimental measurements of light-scattering [8,9]. A comprehensive treatment of Mueller matrix symmetry for single particles and ensembles in fixed and random orientations was performed by van de Hulst [10]. It was further extended by Hovenier and van der Mee [11] with emphasis on practical tests for simulation or experimental results. Specific tests for horizontally oriented particles were also derived [12].

In this paper I consider the Mueller matrix elements integrated over the whole range of the azimuthal scattering angle. To the best of my knowledge, applications of light-scattering symmetries to such integrals have never been considered before, except for a special case in [13]. Specifically, I consider the following integrals:

$$c_{ij}^{m}(\theta) = \frac{1}{2\pi}\int_0^{2\pi} \mathrm{d}\varphi S_{ij}(\theta,\varphi)\cos(m\varphi),$$
$$s_{ij}^{m}(\theta) = \frac{1}{2\pi}\int_0^{2\pi} \mathrm{d}\varphi S_{ij}(\theta,\varphi)\sin(m\varphi), \quad (1)$$

where m is an integer, θ and φ are the polar and azimuthal scattering angles respective to the incident direction, that is further assumed to be along the positive z-axis. S_{ij} is the Mueller matrix element, defined relative to the scattering plane, containing the incident and scattered direction [4]. In particular, if a particle is symmetric with respect to any rotation over the z-axis, S_{ij} is independent of φ. The integrals, described by Eq. (1), are relevant to flow cytometry. In particular, almost any flow cytometer

* Correspondence address: Institute of Chemical Kinetics and Combustion SB RAS, Institutskaya Str. 3, 630090 Novosibirsk, Russia.
Tel.: +7 383 333 3240; fax: +7 383 330 7350.
E-mail address: yurkin@gmail.com

0022-4073/$ - see front matter © 2012 Elsevier Ltd. All rights reserved.
http://dx.doi.org/10.1016/j.jqsrt.2012.11.023

measures forward scattering of single particles in flow, as an integral of the scattering intensity over a certain solid angle near the forward direction. In some configurations azimuthally-symmetric ring detectors are used [14,15], hence the signal can be expressed in terms of $c_{ij}^0(\theta)$. Sometimes several forward-scattering signals for different ranges of θ are used [16], and similar configurations are employed in optical particle sizers [17].

A variation of flow cytometry, scanning flow cytometry (SFC) [18,19], makes even larger use of integrals in Eq. (1). The central part of the SFC optical system is a spherical mirror, symmetric over the incident laser beam [18]. Thus, all measured signals are integrated over the azimuthal angle. Specific expressions depend upon the polarizing optical elements before and after the measured particle [19]. For example, the latest generation of the SFC measures the following signal [20]:

$$I(\theta)=\int_0^{2\pi}\mathrm{d}\varphi[S_{11}(\theta,\varphi)+S_{14}(\theta,\varphi)+(S_{21}(\theta,\varphi)+S_{24}(\theta,\varphi))\cos2\varphi-(S_{31}(\theta,\varphi)+S_{34}(\theta,\varphi))\sin2\varphi] \quad (2)$$

in a wide range of θ. It can be expressed in terms of $c_{ij}^0(\theta)$, $c_{ij}^2(\theta)$, and $s_{ij}^2(\theta)$, while expressions, involving $c_{ij}^4(\theta)$ and $s_{ij}^4(\theta)$, may occur in future versions of the SFC [19]. That is why the discrete-dipole-approximation (DDA, [21]) code ADDA [22] includes functionality to automatically calculate $c_{ij}^{0,2,4}(\theta)$ and $s_{ij}^{2,4}(\theta)$ for a single particle of arbitrary shape and composition.

Another possible utility of Eq. (1) comes from the following combinations:

$$a_{ij}^m(\theta)=\frac{1}{2\pi}\int_0^{2\pi}\mathrm{d}\varphi S_{ij}(\theta,\varphi)\exp(\mathrm{i}m\varphi)=c_{ij}^m(\theta)+\mathrm{i}s_{ij}^m(\theta), \quad (3)$$

which can be considered as Fourier harmonics of the 2D light-scattering patterns (LSPs). Moreover, it is an intermediate step to obtain expansion coefficients of $S_{ij}(\theta,\varphi)$ in terms of the scalar spherical harmonics $Y_{lm}(\theta,\varphi)$

$$b_{ij}^{lm}=\oint\mathrm{d}\Omega S_{ij}(\theta,\varphi)Y_{lm}^*(\theta,\varphi)=N_l\int_0^{\pi}\mathrm{d}\theta a_{ij}^{m*}(\theta)d_{m0}^l(\theta) \quad (4)$$

where $d_{m0}^l(\theta)$ is the Wigner d-function, N_l the normalization constant, and $*$ denotes complex conjugation (see e.g. [23]). Coefficients $a_{ij}^m(\theta)$ and b_{ij}^{lm} can be used to compress 2D LSPs calculated on a grid of scattering angles into a (smaller) set of numbers. Moreover, these coefficients can potentially be directly computed, without $S_{ij}(\theta,\varphi)$ themselves, by some of the light-scattering methods, such as the T-matrix method [23].

The goal of this paper is to analyze the effect of certain particle symmetries on Eqs. (1) and (3) both to derive tests for verification of numerical simulations and/or experimental measurements and to improve the brute-force computation of these integrals by the light-scattering codes. To verify theoretical conclusions I also present several sample simulations with the DDA.

2. Symmetry of a particle in a fixed orientation

Keeping the SFC applications in mind, I limit myself to the symmetries which are relevant for a fixed value of θ. This generally omits the reciprocity, rotational symmetry around other than the z-axis, and symmetry planes not containing the z-axis. However, the following trivial relations always hold:

$$c_{ij}^m(\theta)=c_{ij}^{-m}(\theta),\ s_{ij}^m(\theta)=-s_{ij}^{-m}(\theta),\ a_{ij}^m(\theta)=a_{ij}^{-m*}(\theta). \quad (5)$$

Let me further consider a particle that is symmetric over the plane $\varphi=\varphi_0$, which scatters light incident along the z-axis. Compare two scattering directions characterized by angles $(\theta,\varphi_0+\varphi)$ and $(\theta,\varphi_0-\varphi)$. Let us denote the amplitude scattering matrices in these directions by S_a and S_a' and Mueller matrices—by S and S' respectively. Scattering configurations $(\theta,\varphi_0+\varphi)$ and $(\theta,\varphi_0-\varphi)$ are completely mirror-symmetric, for which van de Hulst showed [10] that amplitude matrices differ only in signs of the off-diagonal elements:

$$S_a'=\begin{pmatrix}S_2' & S_3'\\ S_4' & S_1'\end{pmatrix}=\begin{pmatrix}S_2 & -S_3\\ -S_4 & S_1\end{pmatrix} \quad (6)$$

employing transformation of the amplitude matrix into the Mueller one (see e.g. [4]) and Eq. (6) one may easily obtain that S and S' differ only in signs of the off-block-diagonal elements:

$$S'=\begin{pmatrix}S_{11}' & S_{12}' & S_{13}' & S_{14}'\\ S_{21}' & S_{22}' & S_{23}' & S_{24}'\\ S_{31}' & S_{32}' & S_{33}' & S_{34}'\\ S_{41}' & S_{42}' & S_{43}' & S_{44}'\end{pmatrix}=\begin{pmatrix}S_{11} & S_{12} & -S_{13} & -S_{14}\\ S_{21} & S_{22} & -S_{23} & -S_{24}\\ -S_{31} & -S_{32} & S_{33} & S_{34}\\ -S_{41} & -S_{42} & S_{43} & S_{44}\end{pmatrix}, \quad (7)$$

or equivalently

$$S_{ij}(\theta,\varphi_0+\varphi)=S_{ij}(\theta,\varphi_0-\varphi)\times\begin{cases}1, & \{i,j\}\in\mathrm{BD}\\ -1, & \{i,j\}\notin\mathrm{BD}\end{cases}, \quad (8)$$

where BD stands for block-diagonal, i.e. either both $i,j\le2$ or both $i,j\ge3$. This corollary of the existence of plane of symmetry was also derived in [12]. Splitting the integration range in Eq. (3) into $[\varphi_0,\varphi_0+\pi]$ and $[\varphi_0+\pi,\varphi_0+2\pi]$ and using Eq. (8) for the second range, one can obtain:

$$a_{ij}^m(\theta)=\frac{\exp(\mathrm{i}m\varphi_0)}{\pi}\int_{\varphi_0}^{\varphi_0+\pi}\mathrm{d}\varphi S_{ij}(\theta,\varphi)\times\begin{cases}\cos[m(\varphi-\varphi_0)], & \{i,j\}\in\mathrm{BD}\\ \mathrm{i}\sin[m(\varphi-\varphi_0)], & \{i,j\}\notin\mathrm{BD}\end{cases}, \quad (9)$$

which, in turn, implies that

$$c_{ij}^m(\theta)=s_{ij}^m(\theta)\times\begin{cases}\cot(m\varphi_0), & \{i,j\}\in\mathrm{BD}\\ -\tan(m\varphi_0), & \{i,j\}\notin\mathrm{BD}\end{cases}. \quad (10)$$

Symmetry implications are especially simple for $\varphi_0=0$, i.e. for the symmetry with respect to the xz-plane (Fig. 1(a)):

$$c_{ij}^m(\theta)=\begin{cases}\frac{1}{\pi}\int_0^{\pi}\mathrm{d}\varphi S_{ij}(\theta,\varphi)\cos(m\varphi), & \{i,j\}\in\mathrm{BD};\\ 0, & \{i,j\}\notin\mathrm{BD}.\end{cases} \quad (11)$$

$$s_{ij}^m(\theta)=\begin{cases}0, & \{i,j\}\in\mathrm{BD};\\ \frac{1}{\pi}\int_0^{\pi}\mathrm{d}\varphi S_{ij}(\theta,\varphi)\sin(m\varphi), & \{i,j\}\notin\mathrm{BD}\end{cases} \quad (12)$$

Eqs. (11) and (12) allow one to reduce the number of calculations for averaging Mueller matrix elements over the azimuthal angle (with different weighting functions) – half of the integrals need not to be evaluated at all, while the rest – only require evaluation through half of the azimuthal range.

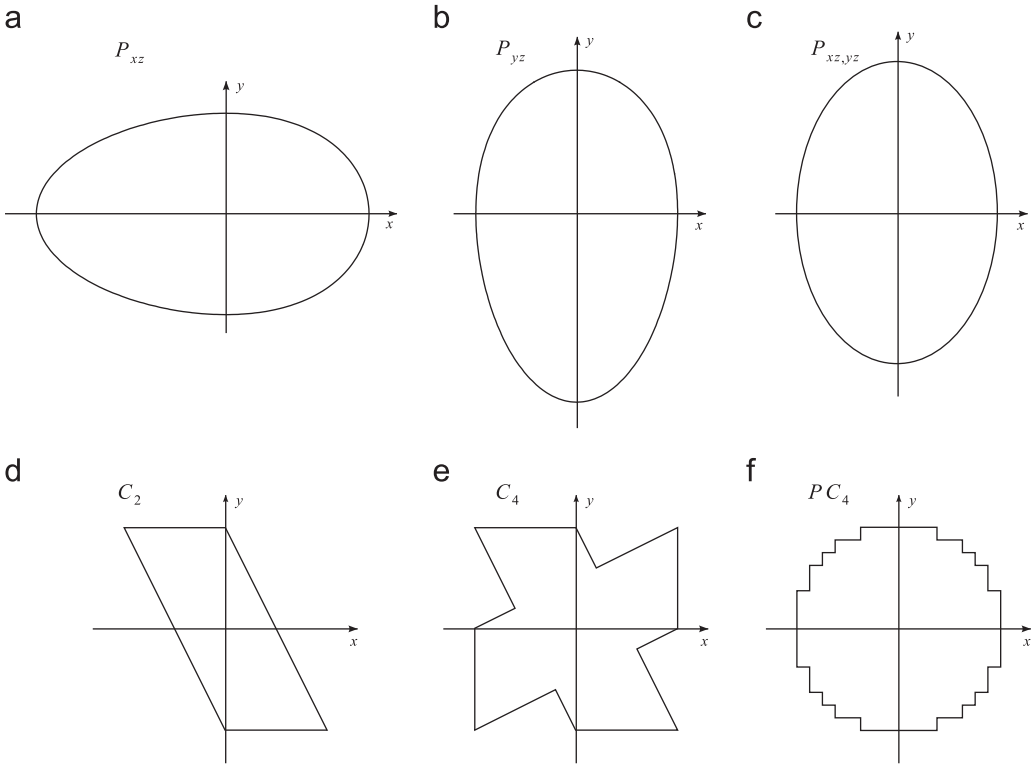

Fig. 1. Examples of considered symmetries, as projections on the *xy*-plane. See the text for description of particular implementations used for the DDA simulations.

Table 1
Implications of different symmetries for the integrals $c_{ij}^m(\theta)$ and $s_{ij}^m(\theta)$. Examples of these symmetries are given in Fig. 1. "0" corresponds to the zero value of the integral, while "1" indicates that the corresponding integral is equal (with appropriate scaling) to the one computed over the reduced range. See the text for details.

Sym.		$\{i,j\}\in$ BD								$\{i,j\}\notin$ BD							
	$m=$	$4k$		$4k+1$		$4k+2$		$4k+3$		$4k$		$4k+1$		$4k+2$		$4k+3$	
	Range	c	s	c	s	c	s	c	s	c	s	c	s	c	s	c	s
P_{xz}	$[0;\pi]$	1	0	1	0	1	0	1	0	0	1	0	1	0	1	0	1
P_{yz}	$[-\pi/2;\pi/2]$	1	0	0	1	1	0	0	1	0	1	1	0	0	1	1	0
$P_{xz,yz}$	$[0;\pi/2]$	1	0	0	0	1	0	0	0	0	1	0	0	0	1	0	0
C_2	$[0;\pi]$	1	1	0	0	1	1	0	0	1	1	0	0	1	1	0	0
C_4	$[0;\pi/2]$	1	1	0	0	0	0	0	0	1	1	0	0	0	0	0	0
PC_4	$[0;\pi/4]$	1	0	0	0	0	0	0	0	0	1	0	0	0	0	0	0

Moreover, these relations are summarized in Table 1 in the row labeled P_{xz}. The table distinguishes block-diagonal (BD) and other elements of the Mueller matrix, different values of m modulo 4, and cosine (c) and sine (s) integrals.

Let me outline the derivation of symmetry relations for other symmetries given in Table 1, examples of which are depicted in Fig. 1. Symmetry with respect to the *yz*-plane (P_{yz}, Fig. 1(b)) is considered based on Eq. (9) for $\varphi_0=-\pi/2$. Contrary to P_{xz}, the result depends on the parity of m. $P_{xz,yz}$ (Fig. 1(c)) denotes a combination of both P_{xz} and P_{yz}; the corresponding row in Table 1 is obtained by element-wise multiplication of that for P_{xz} and for P_{yz}. C_2 and C_4 denote the second- and fourth-order rotational symmetry over the *z*-axis, respectively (Fig. 1(d and e)). For C_2 symmetry $S_{ij}(\theta,\varphi)=S_{ij}(\theta,\varphi+\pi)$ because the corresponding operation rotates the scattering plane as a whole. Therefore, splitting the integration range in Eq. (3) into $[0,\pi]$ and $[0,2\pi]$, one can obtain

$$a_{ij}^m(\theta)=\frac{1+\exp(im\pi)}{2\pi}\int_0^\pi d\varphi S_{ij}(\theta,\varphi)\exp(im\varphi), \qquad (13)$$

in particular, the integrals vanish for odd m. Analogously, for C_4 symmetry the integrals vanish when $m\neq 4k$. Symmetry PC_4 is a combination of C_4 with either P_{xz} or P_{yz}. It often appears in practical applications; for instance, it is realized for any axisymmetric (over the *z*-axis) particle that is

Table 2
Same as Table 1 but for the integrals $a_{ij}^m(\theta)$, and hence for b_{ij}^{lm}. "Re" and "Im" denotes purely real and imaginary values, while "X" is a general complex value.

Sym.	$\{i,j\}\in$BD				$\{i,j\}\notin$BD			
	$m=4k$	$m=4k+1$	$m=4k+2$	$m=4k+3$	$m=4k$	$m=4k+1$	$m=4k+2$	$m=4k+3$
P_{xz}	Re	Re	Re	Re	Im	Im	Im	Im
P_{yz}	Re	Im	Re	Im	Im	Re	Im	Re
$P_{xz,yz}$	Re	0	Re	0	Im	0	Im	0
C_2	X	0	X	0	X	0	X	0
C_4	X	0	0	0	X	0	0	0
PC_4	Re	0	0	0	Im	0	0	0

symmetrically discretized into the dipoles by a DDA code, see e.g. Fig. 1(f).

Finally, all the relations summarized in Table 1 can be recast in terms of $a_{ij}^m(\theta)$, which in certain cases is bound to be zero or purely real or imaginary—see Table 2. The added value is that these symmetry implications are independent of θ and, hence, apply to the coefficients b_{ij}^{lm} as well (cf. Eq. (4)).

3. Euler angles

Many particle symmetries best conform to the coordinate axes when the particle is in the default orientation, i.e. when the particle reference frame coincides with the laboratory one. In general, a rotated particle can be treated by methods developed in Section 2 according to its remaining symmetry with respect to the laboratory reference frame. However, a couple of specific examples are considered below. Particle orientation can be defined by three Euler angles (α,β,γ), which transform the laboratory reference frame into the particle one. The default orientation corresponds to $\alpha=\beta=\gamma=0$. Although a variety of Euler angles definitions exist,[1] the "*zyz*-notation" (or "*y*-convention") is assumed in this paper, as used in several light-scattering codes [22,24].

First, let me consider the effect of the Euler angle α. When incident light propagates along the z-axis the following two scattering problems are completely equivalent: a particle with Euler angles (α,β,γ) scattering at (θ,φ) and a particle $(0,\beta,\gamma)$ scattering at $(\theta,\ \varphi-\alpha)$, i.e.

$$S(\theta,\varphi,\alpha,\beta,\gamma)=S(\theta,\varphi-\alpha,0,\beta,\gamma), \tag{14}$$

this in combination with substituting the variable of integration leads to

$$a_{ij}^m(\theta,\alpha,\beta,\gamma)=\exp(\mathrm{i}m\alpha)a_{ij}^m(\theta,0,\beta,\gamma), \tag{15}$$

which can be separated into real and imaginary parts as

$$c_{ij}^m(\theta,\alpha,\beta,\gamma)=\cos(m\alpha)c_{ij}^m(\theta,0,\beta,\gamma) -\sin(m\alpha)s_{ij}^m(\theta,0,\beta,\gamma), \tag{16}$$

$$s_{ij}^m(\theta,\alpha,\beta,\gamma)=\sin(m\alpha)c_{ij}^m(\theta,0,\beta,\gamma) +\cos(m\alpha)s_{ij}^m(\theta,0,\beta,\gamma), \tag{17}$$

[1] http://en.wikipedia.org/wiki/Euler_angles.

respectively. Although the integrals do depend on α (except when $m=0$), their values for any α can be trivially obtained from a single simulation for, e.g., $\alpha=0$. It should be noted, however, that this simplification is not unique to integrated light-scattering quantities. Rather it is a consequence of general symmetry given by Eq. (14), which is widely used to reduce numerical effort when performing orientation averaging [25,26].

Euler angles β and γ do not allow for simple relations like Eq. (14), since they affect the incident direction in the particle reference frame. However, there is a simple specific case—an axisymmetric particle with the symmetry axis coinciding with the z-axis in the default orientation. Then angle γ is redundant, and only $\alpha=0$ need to be simulated (see above). Moreover, for any value of β the particle is symmetric over the xz-plane; therefore all relations from Section 2 corresponding to P_{xz} apply.

4. Numerical tests

The relations, given in Section 2, allow one to reduce the time for computing the integrals of the Mueller matrix by several times. In this section a number of light-scattering simulations are performed to test the theoretical conclusions and to show the typical level of inaccuracy of the symmetry relations in the framework of the DDA. All simulations are performed with the DDA code ADDA 1.1 [22], adjusted to show 16 significant digits in the produced Mueller matrix values instead of the default 10. I used the default simulation parameters: the polarizability formulation lattice dispersion relation, iterative solver quasi-minimal residual with convergence threshold 10^{-5}, refractive index 1.5, and 15 dipoles per wavelength in vacuum.

One test particle was chosen for each of the considered symmetries; their cross-sections in the xy-plane are shown in Fig. 1. In particular, the P_{xz} and P_{yz} examples are given by an axisymmetric egg, rotated by the Euler angles $\{\alpha,\beta\}=\{0^\circ,90^\circ\}$ and $\{90^\circ,90^\circ\}$ respectively. This particular egg is defined by ADDA command line option "-egg 1 0.9". The $P_{xz,yz}$ example is an oblate spheroid with aspect ratio 2:3 and symmetric over the x-axis. C_2 and C_4 examples are right prisms with base faces shown in Fig. 1(d) and (e), respectively, and equal widths along all three axes. Finally, PC_4 example is a sphere, which is equivalent to its cubical discretization (Fig. 1(f)) with respect to the DDA simulation [22]. For all particles the size was chosen so that exactly 16

Table 3
DDA simulation results for the integrals $c_{ij}^m(\theta)$ and $s_{ij}^m(\theta)$ depending on the particle symmetries. Shown are the minimum (over θ, i, and j) numbers of correct (zero) decimal digits, i.e. $-\log(x)$ rounded to the nearest integer. Values given in standard typeface correspond to the absolute values of the integrals, while values in bold—to the difference between the value of the integral for the full and reduced ranges of φ (see Table 1), both relative to $c_{11}^0(\theta)$. See the text for details.

	$\{i,j\}\in$ BD								$\{i,j\}\notin$ BD							
$m=$	{0,4}		1		2		3		{0,4}		1		2		3	
Sym.	c	s	c	s	c	S	c	s	c	s	c	s	c	s	c	s
P_{xz}	**12**	12	**12**	12	**12**	12	**12**	12	12	**12**	12	**12**	12	**12**	12	**12**
P_{yz}	**12**	12	12	**12**	**12**	12	12	**12**	12	**12**	**12**	12	12	**12**	**12**	12
$P_{xz,yz}$	**8**	8	9	9	**8**	8	8	9	8	**8**	9	8	8	**8**	9	8
C_2	**15**	**15**	15	15	**15**	**15**	15	15	**15**	**15**	15	15	**15**	**15**	15	15
C_4	**11**	**11**	13	13	10	11	13	13	**10**	**11**	13	13	11	10	13	13
PC_4	**8**	14	11	11	8	12	12	13	11	**8**	11	11	12	8	13	13

dipoles fit into the width along the x- and y-axes (whichever of the two is the smallest).

The complete Mueller matrix was calculated on a regular grid of scattering angles θ and φ covering the full solid angle with steps of 2° and 5.625° respectively. A simple Mathematica program was created to perform the integration over φ using the trapezoidal rule (for both full and reduced ranges), which coincides with the procedure used in ADDA for periodic functions. To test the correctness of this program I compared the results for $c_{ij}^{0,2,4}(\theta)$ and $s_{ij}^{2,4}(\theta)$ against the values separately produced by ADDA, using command line option "-phi_integr 31" [22]. The difference divided by $c_{11}^0(\theta)$ was always smaller than 5×10^{-16}. It is important to note that the chosen set of φ values satisfies all considered symmetries and contains intermediate angles, such as 45°. Hence, the trapezoidal sum should satisfy the relations implied by analysis of Section 2, irrespective of its accuracy in approximating the integral itself.

For each test particle the integrals $c_{ij}^{0-4}(\theta)$ and $s_{ij}^{1-4}(\theta)$ were computed for every θ using the full $[0,2\pi]$ and reduced ranges of φ (see Table 1). These values were further divided by $c_{11}^0(\theta)$ to make a fairer comparison between different tests. I found an exact agreement of simulations with Table 1. In particular, the computed integrals or difference between the integrals computed for the full or reduced ranges of φ are negligibly small if and only if the corresponding entry in Table 1 is 0 or 1 respectively. A more quantitative summary is given by Table 3, showing the number of correct digits for both these measures (the more, the better). The minimum is 8 digits, which occurs for the highest-order symmetries (PC_4 and $P_{xz,yz}$). That is expected due to accumulation of round-off errors, but the particular values depend complexly on the parameters of the DDA simulations. The detailed analysis of this dependence lies outside the scope of this paper; the current summary is that the default ADDA parameters lead to more-than-sufficient accuracy. Such a good accuracy can be explained by the fact that the discretization, which is equivalent to replacing the particle with a set of point dipoles, does not break any symmetry from Table 1. Thus, the computed Mueller matrix should satisfy the corresponding symmetry relations, irrespective of the DDA accuracy itself; the latter being mostly determined by the discretization level. This is completely analogous to very good reciprocity accuracy in the DDA [6].

It is instructive to also consider an even simpler option to calculate these integrals for a sphere, which is to assume the full azimuthal rotational symmetry of the DDA results. Then the only relevant integral is $c_{ij}^0(\theta)\approx S_{ij}(\theta,\varphi)$, which can be computed for any fixed φ (a single scattering plane). The only drawback is that the result slightly depends on φ, varying around the rigorously computed (integrated) value of $c_{ij}^0(\theta)$. On the one hand, this variation is significantly smaller than the error of the DDA results for S_{11} (in comparison with the Mie theory), at least for the specific simulation performed in this paper (data not shown). On the other hand, non-zero albeit small values of non-BD elements of $c_{ij}^0(\theta)$ may cause problems in certain applications. Therefore, rigorously computed $c_{ij}^0(\theta)$, e.g. by the integral over the reduced range of φ, is a more adequate (more symmetric), if not necessarily more accurate, estimate of $S_{ij}(\theta)$ for an axisymmetric particle.

Finally, it is important to note, that the vanishing integrals do not generally vanish when computed over the reduced range of φ (as implied by "if and only if" statement above). Thus, when computing a specific experimental signal, e.g. Eq. (2), with an existing code one should not only reduce the integration range, but also manually discard the vanishing terms.

5. Conclusion

Starting from the known symmetry relations for the Mueller matrices at different scattering angles, I have derived explicit symmetry relations for the azimuthal Fourier components of the Mueller matrix. Depending on the scatterer symmetries and order of sine or cosine components, a component either vanishes or equals the one computed over the reduced angular range. First, this provides an independent test for any computer code that computes these quantities. This was illustrated by the DDA simulations, which satisfied all these relations with at least 8 correct significant digits (for the default parameters used in ADDA code). Second, the symmetry relations allow one to reduce the time for computing the integrals of

the Mueller matrix for a symmetric particle by several times. However, computing the Mueller matrix at a set of scattering angles is only a part of a light-scattering simulation, and the relative computational burden depends on the particular scattering problem. For instance, it may be negligibly small for metallic nanoparticles [27] but takes more than half of the total simulation time for large biological cells in water [28].

Acknowledgments

I thank Konstantin Gilev, Alexander Moskalensky, and Anastasiya Konokhova for inspiring discussions and anonymous reviewer for helpful comments. This research was supported by the program of the Russian Government "Research and educational personnel of innovative Russia" (Contracts 8752 and 8804), by Grant from the Russian Government 11.G34.31.0034, and by the Russian Foundation of Basic Research (Grant 12-04-00737-a).

References

[1] Mie G. Beitrage zur optik truber medien, speziell kolloidaler metallosungen. Ann Phys 1908;330:377–445.
[2] Yurkin MA, Kahnert M. Light scattering by a cube: accuracy limits of the discrete dipole approximation and the T-matrix method. J Quant Spectrosc Radiat Transfer. http://dx.doi.org/10.1016/j.jqsrt.2012.10.001; in press.
[3] Kahnert M. T-matrix computations for particles with high-order finite symmetries. J Quant Spectrosc Radiat Transfer. http://dx.doi.org/10.1016/j.jqsrt.2012.08.004; in press.
[4] Bohren CF, Huffman DR. Absorption and scattering of light by small particles. New York: Wiley; 1983.
[5] Rother T, Wauer J. Case study about the accuracy behavior of three different T-matrix methods. Appl Opt 2010;49:5746–56.
[6] Schmidt K, Yurkin MA, Kahnert M. A case study on the reciprocity in light scattering computations. Opt Express 2012;20:23253–74.
[7] Brown AJ, Xie Y. Symmetry relations revealed in Mueller matrix hemispherical maps. J Quant Spectrosc Radiat Transfer 2012;113:644–51.
[8] Hovenier JW. Measuring scattering matrices of small particles at optical wavelengths. In: Mishchenko MI, Hovenier JW, Travis LD, editors. Light scattering by nonspherical particles, theory, measurements, and applications. New York: Academic Press; 2000. p. 355–65.
[9] Munoz O, Moreno F, Guirado D, Ramos JL, López A, Girela F, et al. Experimental determination of scattering matrices of dust particles at visible wavelengths: the IAA light scattering apparatus. J Quant Spectrosc Radiat Transfer 2010;111:187–96.
[10] van de Hulst HC. Light scattering by small particles. New York: Dover; 1981.
[11] Hovenier JW, van der Mee CVM. Testing scattering matrices: a compendium of recipes. J Quant Spectrosc Radiat Transfer 1996;55:649–61.
[12] Hovenier JW, Muñoz O. Symmetry relations for the phase matrix of horizontally oriented particles. J Quant Spectrosc Radiat Transfer 2010;111:1449–53.
[13] Yurkin MA, Semyanov KA, Tarasov PA, Chernyshev AV, Hoekstra AG, Maltsev VP. Experimental and theoretical study of light scattering by individual mature red blood cells with scanning flow cytometry and discrete dipole approximation. Appl Opt 2005;44:5249–56.
[14] Salzman GC, Singham SB, Johnston RG, Bohren CF. Light scattering and cytometry. In: Melamed MR, Lindmo T, Mendelson ML, editors. Flow cytometry and sorting. 2nd ed. New York: Wiley–Liss; 1990. p. 81–107.
[15] Givan AL. Flow cytometry: first principles. 2nd ed.New York: Wiley–Liss; 2001.
[16] Rajwa B, Venkatapathi M, Ragheb K, Banada PP, Hirleman ED, Lary T, et al. Automated classification of bacterial particles in flow by multiangle scatter measurement and support vector machine classifier. Cytometry A 2008;73:369–79.
[17] Szymanski WW, Nagy A, Czitrovszky A. Optical particle spectrometry—problems and prospects. J Quant Spectrosc Radiat Transfer 2009;110:918–29.
[18] Maltsev VP. Scanning flow cytometry for individual particle analysis. Rev Sci Instrum 2000;71:243–55.
[19] Maltsev VP, Semyanov KA. Characterisation of bio-particles from light scattering.Utrecht: VSP; 2004.
[20] Strokotov DI, Moskalensky AE, Nekrasov VM, Maltsev VP. Polarized light-scattering profile—advanced characterization of nonspherical particles with scanning flow cytometry. Cytometry A 2011;79A:570–9.
[21] Yurkin MA, Hoekstra AG. The discrete dipole approximation: an overview and recent developments. J Quant Spectrosc Radiat Transfer 2007;106:558–89.
[22] Yurkin MA, Hoekstra AG. The discrete-dipole-approximation code ADDA: capabilities and known limitations. J Quant Spectrosc Radiat Transfer 2011;112:2234–47.
[23] Mishchenko MI, Travis LD, Lacis AA. Scattering, absorption, and emission of light by small particles.Cambridge: Cambridge University Press; 2002.
[24] Mishchenko MI. Calculation of the amplitude matrix for a nonspherical particle in a fixed orientation. Appl Opt 2000;39:1026–31.
[25] Penttila A, Zubko E, Lumme K, Muinonen K, Yurkin MA, Draine BT, et al. Comparison between discrete dipole implementations and exact techniques. J Quant Spectrosc Radiat Transfer 2007;106:417–36.
[26] Penttilä A, Lumme K. Optimal cubature on the sphere and other orientation averaging schemes. J Quant Spectrosc Radiat Transfer 2011;112:1741–6.
[27] Yurkin MA, De Kanter D, Hoekstra AG. Accuracy of the discrete dipole approximation for simulation of optical properties of gold nanoparticles. J Nanophoton 2010;4:041585.
[28] Orlova DY, Yurkin MA, Hoekstra AG, Maltsev VP. Light scattering by neutrophils: model, simulation, and experiment. J Biomed Opt 2008;13:054057.